

Evaluation of Spatial Correlation between Nutrient Exchange Rates and Benthic Biota in a Reef-Flat Ecosystem by GIS-Assisted Flow-Tracking

TOSHIHIRO MIYAJIMA^{1*}, YOSHIYUKI TANAKA¹, ISAO KOIKE¹, HIROYA YAMANO^{2†}
and HAJIME KAYANNE²

¹Department of Chemical Oceanography, Ocean Research Institute, The University of Tokyo,
Minamidai, Nakano-ku, Tokyo 164-8639, Japan

²Department of Earth and Planetary Science, Graduate School of Science, The University of Tokyo,
Hongo, Bunkyo-ku, Tokyo 113-0033, Japan

(Received 21 July 2006; in revised form 1 February 2007; accepted 10 March 2007)

A Geographic Information System (GIS)-aided flow-tracking technique was adopted to investigate nutrient exchange rates between specific benthic communities and overlying seawater in a fringing reef of Ishigaki Island, subtropical Northwestern Pacific. Net exchange rates of NO_3^- , NO_2^- , NH_4^+ , PO_4^{3-} , Total-N and Total-P were estimated from concentration changes along the drogoue trajectories, each of which was tracked by the Global Positioning System and plotted on a benthic map to determine the types of benthic habitat over which the drogoue had passed. The observed nutrient exchange rates were compared between 5 typical benthic zones (branched-coral (B) and *Heliopora* communities (H), seaweed-reefrock zone (W), bare sand area (S), and seagrass meadow (G)). The dependence of nutrient exchange rates on nutrient concentrations, physical conditions and benthic characteristics was analyzed by multiple regression analysis with the aid of GIS. The spatial correlation between nutrient exchange rates and benthic characteristics was confirmed, especially for NO_3^- and PO_4^{3-} , which were usually absorbed in hydrographically upstream zones B and W and regenerated in downstream zones H and G. NO_3^- uptake in zones B and W was concentration-dependent, and the uptake rate coefficient was estimated to be 0.58 and 0.67 m h^{-1} , respectively. Both nutrient uptake in zone W and regeneration in zone H were enhanced in summer. The net regeneration ratio of $\text{NO}_3^-/\text{PO}_4^{3-}$ in zone H in summer ranged 5.2 to 34 (mean, 17.4), which was somewhat higher than previously measured $\text{NO}_3^-/\text{PO}_4^{3-}$ for sediment pore waters around this zone (1.1–8.5). Nutrient exchanges in zone S were relatively small, indicating semi-closed nutrient cycling at the sediment-water interface of this zone. NH_4^+ efflux from sediments was suggested in zone G. The data suggest that the spatial pattern of nutrient dynamics over the reef flat community was constrained by zonation of benthic biota, and that abiotic factors such as nutrient concentrations and flow rates, influenced nutrient exchange rates only in absorption-dominated communities such as zones B and W.

Keywords:

- Nutrient flux,
- benthic macrophytes,
- coral reef,
- Geographic Information System (GIS),
- nitrate,
- phosphate,
- silicate.

1. Introduction

Coral reefs are macrobenthos-dominated ecosystems in tropical and subtropical coastal seas, where seawater constantly flows over benthic biota and exchange of nu-

trients such as nitrogen (N), phosphorus (P) and silicon (Si) occurs predominantly between benthic biota and overlying water. A coral reef ecosystem is often segmented into several distinct zonal communities (Odum and Odum, 1955; Wiebe, 1988), which include patchy hermatypic coral communities, exposed reefrocks with algal turfs and macroalgae, and sanded flat harboring an epipsamic microalgal community, calcareous algal (e.g., *Halimeda*) beds and seagrass meadows. These communities may differ significantly from each other in optimum ambient

* Corresponding author. E-mail: miyajima@ori.u-tokyo.ac.jp

† Present address: National Institute for Environmental Studies, Onogawa, Tsukuba, Ibaraki 305-8506, Japan.

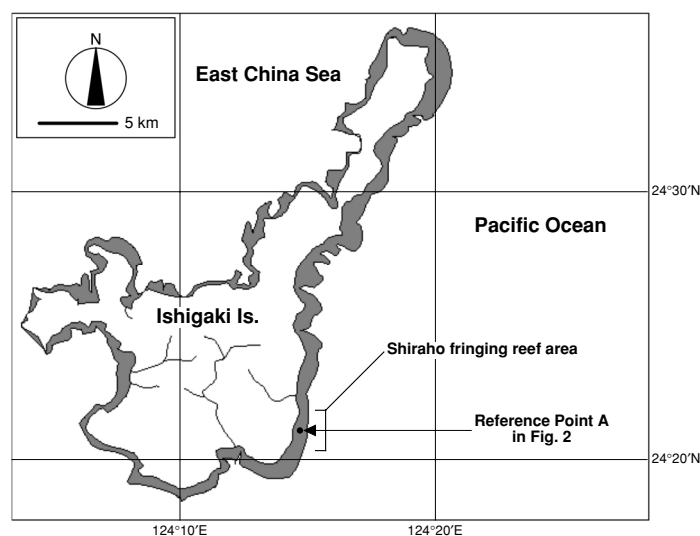


Fig. 1. Map of Ishigaki Island and location of the study site, Shiraho fringing reef. Gray area is fringing reefs around the island.

concentration and uptake affinity for specific dissolved nutrients. Such differences can play important roles in determining the spatial distribution of respective communities, and consequently, overall metabolic performance of the entire reef ecosystem.

Recent studies have demonstrated that acquisition of dissolved nutrients by the coral reef biota is limited by mass-transfer rates, and that gross uptake rates of nutrients by individual reef benthos are determined principally by external physico-chemical factors, including water flow velocity, wave-energy input and nutrient concentrations in inflowing ocean waters (Atkinson and Falter, 2003; Falter *et al.*, 2004). The dependence of uptake rate by reef benthos on water motion has been demonstrated for phosphate (PO_4^{3-} ; Atkinson and Bilger, 1992), ammonium (NH_4^+ ; Bilger and Atkinson, 1995; Thomas and Atkinson, 1997) and nitrate (NO_3^- ; Baird *et al.*, 2004) and generalized mathematically by Hearn *et al.* (2001). Concentration-dependent nutrient uptake has also been reported for PO_4^{3-} (D'Elia, 1977; Atkinson, 1987; Sorokin, 1992), NH_4^+ (Burris, 1983; Bilger and Atkinson, 1995; Steven and Atkinson, 2003) and NO_3^- (Bythell, 1990; Tanaka *et al.*, 2006). However, many of these studies employed isolated coral cultures or focused on coral-dominated reef-flat subsystems to demonstrate these relationships. Thus, it is still obscure whether or not similar relationships can be applied to all the different communities within the coral reef ecosystem, and to what degree the mass-transfer limitation constrains the metabolic performance of the whole ecosystem and material exchanges between coral reefs and the surrounding ocean.

Although numerous studies have been carried out to estimate nutrient exchange rates between benthic biota

and seawater over the whole reef system (e.g., Pilson and Betzer, 1973; Webb *et al.*, 1975; Crossland and Barnes, 1983; Johannes *et al.*, 1983; Charpy *et al.*, 1998; Mioche and Cuet, 1999; Baird *et al.*, 2004), spatial correlations between nutrient fluxes and benthic biota within a reef ecosystem have rarely been evaluated successfully. To this end, both precise measurement of temporal changes in nutrient concentrations and detailed, quantitative information on the horizontal distribution of representative benthic communities are needed; the latter has often been absent in previous studies of coral reef biogeochemistry. Benthic metabolic activities under flowing-water conditions have often been measured by the "flow-respirometric" approach, in which a single water mass is tracked using a drogue and chemical properties of the water mass, such as O_2 and pH , are measured over the course of time (e.g., Barnes, 1983; Barnes and Devereux, 1984). However, nutrient studies employing this technique are scarce.

A similar approach has been adopted in the present study: the movement of a water mass over the reef flat of a coral reef was followed by tracking a small submerged drogue, and concentration changes of nutrients in the water mass conveying the drogue were monitored periodically. Net nutrient exchange rates were then calculated from temporal changes in concentrations, and compared between characteristic benthic communities. In an attempt to evaluate quantitatively the relationships between nutrient dynamics and reef flat benthic communities, the benthic biota of the study area has been mapped in terms of both coverage and biomass (C, N, P). The benthic characteristics below the drogue tracks were determined using a Geographic Information System (GIS) program based on the vegetation maps. Physical parameters, in-

cluding water temperature, sea-surface light intensity and water flow, were also monitored simultaneously. Estimated nutrient exchange rates were compared between different benthic zones, and relationships between benthic characteristics and behavior of nutrients were surveyed. Relative influences of benthic types and physico-chemical conditions on nutrient dynamics on the reef flat were also compared using multiple regression analysis.

The aims of this study are to examine: (1) how effectively the proposed technique could detect and quantify spatial correlations of nutrient dynamics; (2) whether and how nutrient dynamics on the reef flat varied depending on benthic biota; and (3) to what extent nutrient exchange rates between individual reef communities and the overlying water were controlled by external physico-chemical factors.

2. Material and Methods

2.1 Study site and vegetation mapping

The study area is a reef flat in the shallow lagoon (depth, 0.5–3.0 m below the mean sea level) of Shiraho coral reef (24°21′–22′ N, 124°15′ E; Fig. 1), east of Ishigaki Island, subtropical NW Pacific (Nakamori *et al.*, 1992; Hata *et al.*, 2002). The general characteristics of nutrient dynamics of this reef have been described elsewhere (Miyajima *et al.*, 2007). The hydrodynamics of the lagoon are strongly restricted by the tidal cycle. This study was carried out only during the high tide periods, because the shallowness of water depth and many emergent coral heads during low tide made it difficult to follow water movement by the drogue experiment. Water current velocity and turnover time in the lagoon during the high tide periods has been estimated as 10–30 cm s⁻¹ and about 3 h, respectively, which can vary depending on tide and swell height in the outer ocean and wind velocity (Yamano *et al.*, unpublished data).

Sessile macrophyte distribution in the lagoon shows a zonal pattern. Patchy seagrass beds occur in the nearshore (i.e. west) part of the lagoon, up to 350 m from the shoreline. Dominant seagrass species are *Thalassia hemprichii*, *Cymodocea rotundata* and *Cymodocea serrulata* (Tanaka and Kayanne, 2006). Small colonies of corals such as *Porites* sp. also occur in this region. Large patches of hermatypic corals occur abundantly in the zone between 500 m and 700 m from the shoreline. Dominant species are *Acropora* spp., *Montipora* spp. and *Porites* spp. in the northern part, and *Heliopora coerulea* in the southern part. A large gap zone of macrophytes exists between the seagrass beds and the coral belt. Pristine carbonate sand, predominantly of coral-skeleton origin, covers this area. A number of exposed reefrocks are found in this sanded area as well as in seagrass beds, on which macroalgae develop seasonally. Macroalgae found

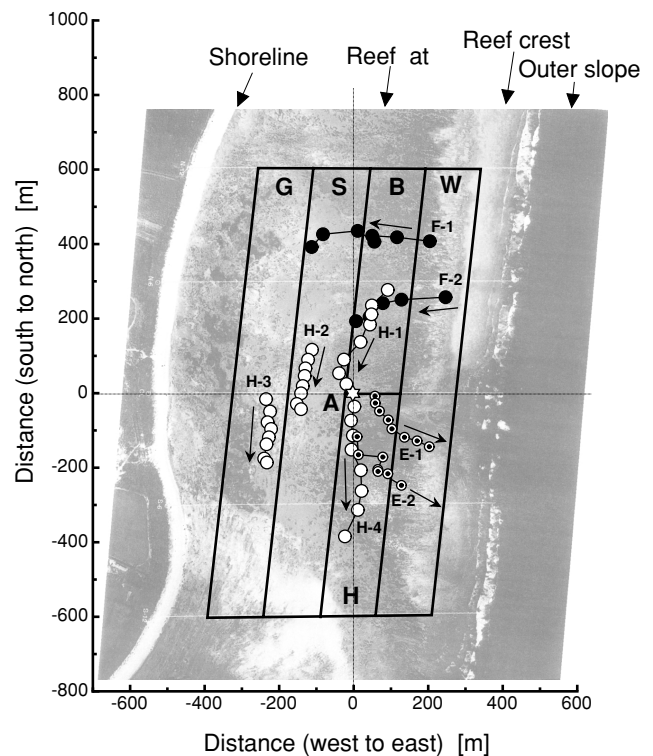


Fig. 2. Aerial photograph of the study site reef flat, with five zones (W, B, H, S, G) plotted parallel to the reef crest. Coverages of representative benthic biota on each zone are shown in Table 1. Point A is the reference point of GPS mapping. Some examples of flow trajectories of drogue experiments (F-1, F-2; H-1, H-2, H-3, H-4; E-1, E-2) are also shown with water sampling points (circles) and flow directions (arrows).

in these regions include brown algae such as *Sargassum* and *Padina*, which mainly grow in summer, and green algae such as *Ulva*, which mainly grow in winter. The bottom of the area >700 m off the shoreline is mostly covered with reefrocks, on which brown algae grow from spring through autumn. During low tide periods, groundwater discharge occurs along the shoreline (Kawahata *et al.*, 2000; Umezawa *et al.*, 2002). Groundwater nutrient concentrations have been estimated as freshwater-endmember concentrations extrapolated from concentration-salinity regression lines obtained in the groundwater-seeping area: NO₃⁻, 263 ± 8 μM; Si(OH)₄, 127 ± 3 μM; NO₂⁻, NH₄⁺ and PO₄³⁻, < 1 μM. Groundwater discharge is reduced during high tide periods due to hydraulic balance.

Based on this zonal pattern, the reef flat has been divided into five zones: branched-coral dominated (B), *Heliopora*-dominated (H), seaweed-reefrock (W), bare sand (S) and seagrass (G) zones (Fig. 2). The coverage of

Table 1. Vegetation in five zones plotted on the reef flat of Shiraho reef. Each zone is 150 m from east to west and 1,200 m (600 m for B and H) from north to south, and placed parallel to the reef crest from offshore to nearshore (see Fig. 2).

Zone	Branched coral zone (B)		<i>Heliopora</i> zone (H)		Seaweed-reefrock zone (W)		Bare sand zone (S)		Seagrass zone (G)	
	90,000	180,000	90,000	180,000	180,000	180,000	180,000	180,000	180,000	180,000
Total area (m ²)										
Coverage (%)										
Coral										
Total	5.8	1.2	5.5	1.2	1.2	1.0	0.9	1.0	0.2	0.8
<i>Acropora</i> + <i>Montipora</i> + branched <i>Porites</i>	5.8	1.0	1.7	1.0	0.2	0.4	0.2	0.0	0.0	0.2
<i>Heliopora</i>	0.0	0.0	3.8	0.2	0.0	0.0	0.2	0.0	0.0	0.0
<i>Pavona</i> + massive <i>Porites</i>	0.0	0.0	0.0	0.0	0.0	0.0	0.0	0.0	0.0	0.0
<i>Sargassum</i>										
(summer)	4.4	43.3	3.3	43.3	0.0	0.0	3.0	3.9	0.2	2.8
(winter)	0.9	1.9	0.0	1.9	0.0	0.0	2.2	0.2	0.0	4.4
Seagrasses										
(summer)	0.0	0.0	0.0	0.0	0.0	0.0	0.2	8.8	0.2	4.4
(winter)	0.0	0.0	0.0	0.0	0.0	0.0	0.2	0.0	0.2	0.0

macrophytes in the respective zones is determined from vegetation maps described below and ranged between 4 and 46% altogether (Table 1).

Vegetation maps of the reef flat were prepared as follows. Benthic biota was classified into five categories: seagrasses, brown algae (represented by *Sargassum*), the octocoral *Heliopora*, branched hermatypic corals (*Montipora* + *Acropora* + branched morphotypes of *Porites*), and massive hermatypic corals (*Pavona* + massive morphotypes of *Porites*). Raster maps of the coverage areas of these categorized communities were prepared first from aerial photographs by image analysis. To estimate biomass from coverage, standing stocks of these organisms were separately determined in 1997 and 1998 for selected quadrats along 5 transects perpendicular to the reef crest with an interval of 300 m. Standing stocks were determined first on a dry-weight basis and then converted into biomass on total organic carbon (TOC), total nitrogen (TN) and total organic phosphorus (TOP) bases using representative TOC, TN and TOP contents of respective macrophytes. In the case of corals, the horizontal distribution map of biomass over the lagoon was prepared from the coverage map using a simple linear relationship between coverage (%) and biomass. Seasonal variation in coral biomass was neglected. In contrast, biomass of *Sargassum* and seagrasses was estimated for respective seasons because they showed significant seasonal variation. Empirical non-linear functions that relate average coverage of *Sargassum* and seagrass to their standing stocks for each season were established to convert the coverage raster maps into the distribution maps of their biomass. The area where none of the above 5 benthic communities occurred was classified into sand-covered zone (near-white pixels) and reefrock-exposed zone (residual area). Consequently, the bottom state of the reef flat was categorized into a total of 7 types. Maps for each of the 7 bottom categories were generated on a 10 m × 10 m grid. The bottom morphology was also expressed by a 10 m × 10 m grid map on which mean depth from mean sea level was plotted for each grid. All the data of bottom-type and depth distributions were incorporated into a tailor-made GIS program.

Due to anomalously high temperature conditions that continued through spring and summer 1998, remarkable coral bleaching occurred over coral reefs in Northwestern Pacific region. In Shiraho reef, branched hermatypic corals such as *Acropora*, *Montipora* and *Porites* were most significantly damaged by bleaching, whereas *Heliopora* and a massive type of *Porites* were little affected. Damaged colonies gradually recovered to the pre-bleaching levels of coverage within two years after the bleaching event, and the present study was conducted during the recovery period. Since the vegetation maps for corals were based on the data of the pre-bleaching period, the biomass

of the affected corals should have been an overestimate to some degree of the actual biomass during the study period. The bleaching event and the recovery process observed in Shiraho reef have been documented in detail by Kayanne *et al.* (2002).

2.2 Water sampling

A small drogue was made of a buoy (15 cm in diameter, 20 cm in length) connected to two polyvinyl-chloride resistance plates (30 cm × 20 cm, one across the other) by a nylon wire. The resistance plates were usually suspended 45 cm below the buoy, although the length was shortened as necessary when the drogue passed through shallower areas. The drogue was released from various locations in the lagoon, and a small boat equipped with a differential Global Positioning System (GPS) instrument followed it closely. Experiments were conducted in the morning (06:30–11:30 Japan Standard Time (JST)) and in the evening (14:00–19:00 JST) of the spring tide periods (cf. the culmination time at the study site is around 12:43 JST). The duration of individual tracks ranged between 18 and 60 min. From the boat, water samples for nutrients (NO_3^- , NO_2^- , NH_4^+ , PO_4^{3-} , Si(OH)_4 ; 10 ml, duplicate) and total nitrogen and phosphorus (TN and TP; 20 ml) were collected in acrylic tubes at 4–10 min intervals using a plastic syringe (50 ml) fitted with a silicone tube and a lead, which enabled seawater to be pumped up from the same depth as the resistance plates. Samples were temporarily stored on ice for transportation, and frozen at -20°C in the laboratory until analysis. In addition, samples for chlorophyll *a* (Chl) determination (200 ml) were also collected at the beginning and the end of each track. At every sampling time, the boat was forced to keep as close to the drogue as possible (usually ~5 m behind), and the location of the boat was recorded using GPS. The onshore station for the differential GPS was set at ca. 1.5 km southwest from the reference point (A in Fig. 2) in the lagoon. The accuracy of GPS outputs (within ± 5 m) was checked by locating the reference point at the beginning and the end of the daily survey. The survey was conducted in 4 seasons and a total of 53 experiments were executed: 1–3 December 1998 (7 experiments), 15–21 March (15), 26–28 June (14) and 23–29 September 1999 (17).

It is assumed that a single water mass flowing across the lagoon could be traced by following a drogue. Movement of the water mass was determined by plotting and interpolating GPS records for the sampling points, from which average water current direction and velocity were calculated. The water mass was assumed to exchange dissolved constituents with the benthic communities beneath its flow trajectory. The benthic community composition that was supposed to influence the flowing water mass was determined by superposing the trajectory on the veg-

etation map with the aid of the GIS.

Physical variables other than water current were measured at the reference point as follows: water temperature (TW) was monitored by a sensor array (H20, HYDROLAB, U.S.A.), sea-surface photosynthetically available radiation (PAR) by a shipboard photon counter (2π cosine-corrected; LI-192SA, Li-Cor, U.S.A.) and water depth by an acoustic Doppler current profiler (Argonaut-XR, SonTek, U.S.A.). Readings of water depth by the profiler were regularly calibrated by comparison with manually measured depth by a scale bar. Spatial variability of TW and PAR was not considered. Water depth along the flow trajectories was determined from real-time depth at the reference point and the difference in bottom height that was estimated from the depth map of the lagoon. Water samples for Chl were filtered through Whatman GF/F filters ($\phi 25$ mm, nominal pore size of $0.7 \mu\text{m}$, precombusted at 450°C for 3 h). The filters were soaked in *N,N*-dimethylformamide (6 ml) in polypropylene tubes and stored at -20°C in the dark for later analysis.

2.3 Measurements of water-column metabolism

Net nutrient exchange rates by planktonic organisms in the water column were estimated by the *in-situ* bottle incubation method. Experiments were conducted 5 times (25 March, 29 and 30 June, 25 and 26 September, 1999). Moat water was pumped up into a 20-l acid-washed polypropylene tank in the morning (flooding periods) on a boat moored at the reference point (A in Fig. 2), and immediately siphoned into 27 glass incubation bottles (inner volume, 100 ml; no air bubbles inside), 4 screw-capped acrylic tubes (10 ml; for initial nutrients, total nitrogen (TN) and total phosphorus (TP)), and a polypropylene bottle (200 ml; for initial Chl). After sampling, the tubes and polypropylene bottle were immediately put on ice for transportation. Three of 27 glass incubation bottles were immediately fixed by the Winkler reagents and stored in a water bath for initial DO measurements. For the other 24 incubation bottles, the cap was tightly fitted with Parafilm-M[®] to prevent water leakage. Among them, 12 bottles were wrapped with aluminum foil to exclude light. Six light and 6 dark bottles were put upside down in each of two cages, and one cage was hung at 80 cm below the water surface, while the other was put on the bottom. The bottles were incubated for 8 h (0900–1700 JST), care being taken that the shadow of the moored boat did not fall on the cages. TW and PAR were monitored as described above. Out of each set of similarly treated 6 incubation bottles, 3 bottles were fixed immediately after incubation by the Winkler reagents, while the other 3 bottles were used for determination of nutrients, TN and TP. The fixed bottles were kept underwater in a bucket until analysis. The samples for nutrient and

TN+TP analyses were transferred from each bottle to 4 acrylic tubes (10 ml; 2 for nutrients and 2 for TN+TP) using a clean autopipette. Water samples in acrylic tubes were stored frozen at -20°C until analysis, while the Winkler titration was carried out within 12 h after the end of incubation. The sample for Chl determination was treated as already described. Oxygen was never depleted in the incubation bottles.

2.4 Chemical analyses and calculations

Since nutrient concentration in seawater flowing across coral reefs is very low and its temporal changes are subtle, great care was paid to avoid contamination throughout surveys and experiments. For sampling, new acrylic tubes and acid-soaked (1 M HCl, overnight) polypropylene bottles were always used, and vigorously washed at least twice with the same seawater as samples prior to sampling. Acid-washed glassware, new and clean pipetter tips, and clean plastic gloves were always employed for filtration and pretreatments for analyses. Stability and sensitivity of analytical instruments were strictly checked.

Concentrations of dissolved nutrients (NO_3^- , NO_2^- , NH_4^+ , PO_4^{3-}) were determined by an AutoAnalyzer AACS-II (BRAN+LUEBBE, Germany). The acrylic tubes that contained frozen seawater samples were thawed and directly sent to the autosampler placed in a clean hood to avoid contamination by atmospheric NH_3 and NO_x . Photometric cells of 50 mm light path were employed, and standard protocols provided by BRAN+LUEBBE Japan were followed. Concentration of dissolved reactive silicate ($\text{Si}(\text{OH})_4$, measured only for September samples) was determined similarly for the samples that were stored at room temperature for at least 24 h after thawing (Burton *et al.*, 1970). Total nitrogen and phosphorus concentrations in seawater were determined simultaneously by the wet oxidation method using a borate-buffered $\text{K}_2\text{S}_2\text{O}_8$ solution (Grasshoff *et al.*, 1999).

Chlorophyll *a* (Chl) concentration was determined by the fluorometric method (Turner Design 10AU) for *N,N*-dimethylformamide in which a 25 mm filter sample had been soaked.

Total organic carbon (TOC) and total nitrogen (TN) contents of dried biological samples were determined by a CHN analyzer (MT-5, Yanaco, Japan) after HCl vapor treatment to remove inorganic carbon. Total organic phosphorus (TOP) was determined for HCl-treated samples by the dry oxidation method using $\text{Mg}(\text{NO}_3)_2$ as catalyst and subsequent colorimetric assay (Suzumura *et al.*, 2002).

The data obtained were statistically analyzed and displayed using software packages StatView ver. 5 (SAS Institute, U.S.A.) and pro Fit ver. 6 (Quantum Soft, Switzerland). Net nutrient exchange rates per unit volume of

flowing water were calculated as linear regression coefficients of nutrient concentrations with tracking time. In the data shown below, net increase in nutrient concentration in the tracked water mass is represented by a positive rate value. Net exchange rate per unit bottom area was calculated for each drogue trajectory by multiplying the average depth (ranging 53–185 cm) with the rate per unit volume.

Observed volume-based exchange rates were examined by stepwise multiple regression analysis (MRA; backward elimination with removal criterion $F < 3$ and entry criterion $F > 4$) for their dependence on various environmental factors. Independent variables included in the analysis are 3 physical variables (TW, PAR, water flow rate), 4 chemical variables (concentrations of NO_3^- , NO_2^- , NH_4^+ , PO_4^{3-}) and 6 benthic variables (areal coverages of sand and reefrocks, areal biomasses of *Sargassum*, seagrasses, *Heliopora*, and the branched corals). Physical and chemical variables are time-average values for each drogue experiment. Concentrations of TN and TP were not used, because the final statistical results never changed significantly by adding them to the independent variables. Water depth was excluded because it significantly correlated with areal reefrock coverage ($r = -0.901$). Areal biomass of the massive corals was also excluded, because it showed strong positive correlation ($r = 0.879$) with areal biomass of seagrasses. Since the dependent variables are volume-based fluxes, coverage and biomass must be corrected for variations of depth. Depth-corrected average coverage or biomass (B) for each drogue trajectory was calculated as follows:

$$B = \frac{1}{T} \int_0^T \frac{b(t)}{d(t)} dt,$$

where t is the time (h) from the start of a track experiment, T is the duration (h) of the experiment, $b(t)$ is the coverage of sand or rock (area %) or the biomass of one of the vegetation categories (mmol-N or P m^{-2}) and $d(t)$ is the depth (m). $b(t)$ and $d(t)$ are given by the GIS database for the $10 \text{ m} \times 10 \text{ m}$ grid in which the drogue stayed at time t . For the biomass, nitrogen- or phosphorus-based estimation was used when the exchange rate to be examined was that of nitrogen or phosphorus, respectively.

3. Results

3.1 Water current characteristics and physical conditions

Some examples of trajectories of the drogue (September 1999) are shown in Fig. 2. Trajectories F-1 and F-2 represent a typical flow pattern during the flood tide periods when water flows from the outer ocean (east) into the lagoon; H-1 to H-4 represent that during the high tide

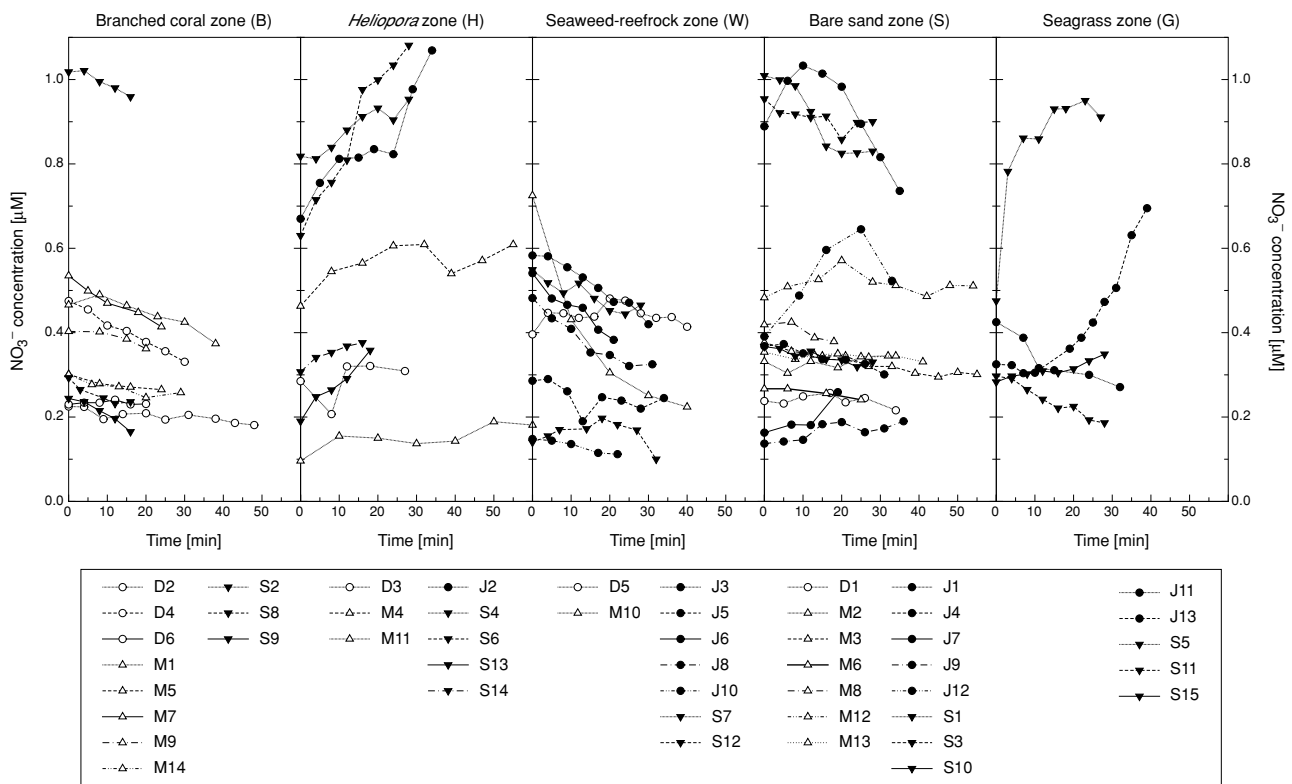


Fig. 3. Temporal changes in NO_3^- concentration during drogue-tracking experiments for five zones defined in Fig. 2. Symbols: open circle, December 1998; open triangle, March 1999; solid circle, June 1999; solid reverse triangle, September 1999. Individual experiments of the same season can be distinguished by lines as shown in the legend.

periods when water flows almost parallel to the reef crest; and E-1 and E-2 represent flow during the ebb tide periods when water flows out of the lagoon. Thus, the component of the flow vector perpendicular to the reef crest depended on the tidal conditions; that is, it was in the direction from offshore landward during the flood tide, and from the lagoon to offshore during the ebb tide. The flow component parallel to the reef crest depended on the prevailing wind direction and the offshore swell state in the NW Pacific Ocean. In many (but not all) cases, this component was in the south-to-north direction during June surveys, and from north to south during December, March and September surveys.

Water temperature was 26.5° – 27.4°C in December, 20.9° – 24.9°C in March, 28.4° – 31.7°C in June, and 27.7° – 28.6°C in September. Average PAR during individual experiments ranged 106 – $478 \mu\text{mol photon m}^{-2} \text{s}^{-1}$ (mean, 283) in December, 63 – 1070 (306) in March, 152 – 1140 (584) in June, and 197 – 1160 (875) in September.

3.2 Nutrient concentrations and net exchange rates in individual zones

Temporal changes in NO_3^- , PO_4^{3-} and Si(OH)_4 during individual drogue-tracking experiments are shown in

Figs. 3 and 4. Si(OH)_4 data are available only for September experiments. In these figures, only those experiments were selected in which the drogue stayed in one of the 5 zones for at least 4 consecutive sampling points ($n = 48$ out of total 53 experiments). For example, concentration data of the first 5 sampling points (zone H) of the experiment E-1 in Fig. 2 are shown, and data for the remaining 3 points (zone W) are discarded; data for the experiment F-1 are not shown, because there were only 1–3 sampling points in any individual zone (W, B, S) during this experiment. Average net exchange rates of inorganic nutrients (except Si(OH)_4), TN and TP per unit bottom area are shown in Fig. 5. Positive rates indicate net increase of concentration in the tracked water mass during experiments.

NO_3^- was usually 0.2 – $0.6 \mu\text{M}$, although concentrations around $1.0 \mu\text{M}$ have been observed in 8 out of 48 experiments. During individual experiments, NO_3^- usually decreased in the branched-coral zone (B) and the seaweed-reefrock zone (W), while it increased in the *Heliopora* zone (H) (Figs. 3 and 5a). In the bare sand zone (S), concentration change was usually small and did not show a consistent trend. In the seagrass zone (G), the pattern of concentration change was highly variable. No

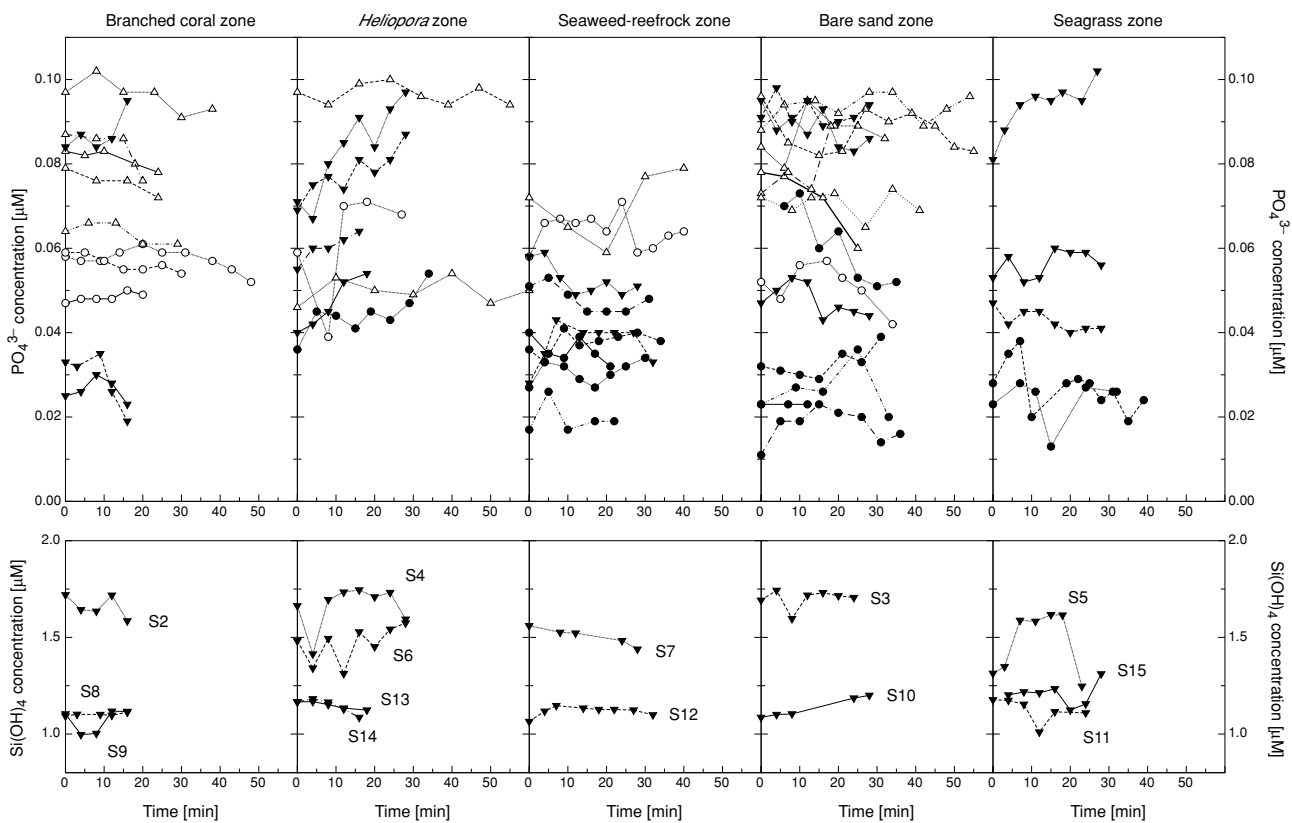


Fig. 4. Temporal changes in PO_4^{3-} (top) and Si(OH)_4 (bottom) concentrations during drogue-tracking experiments. Si(OH)_4 was determined only in September experiments. Symbols are same as Fig. 3.

clear seasonal trend was observed for NO_3^- concentration. On the other hand, NO_2^- was usually $0.03\text{--}0.10\ \mu\text{M}$, and generally higher in September than in the other months. Similarly to NO_3^- , NO_2^- increased in zone H and decreased in zone W (Fig. 5b). However, no consistent temporal pattern of NO_2^- was confirmed in the other zones. NH_4^+ was usually $0.1\text{--}0.4\ \mu\text{M}$ and generally higher in summer (June and September) than in winter (December and March). It often showed a highly complex temporal pattern. Although NH_4^+ increased constantly during some experiments, there was no experiment in which NH_4^+ steadily decreased. On average, NH_4^+ decreased in zone W and increased in zone G (Fig. 5c). PO_4^{3-} was usually $0.02\text{--}0.10\ \mu\text{M}$ and on average, it was higher in March than in the other months (Fig. 4). Similarly to NO_3^- , PO_4^{3-} often decreased in the experiments carried out in zone B and increased in zone H (Fig. 5d). In zones S and G, PO_4^{3-} showed no consistent temporal pattern. Total N concentration was usually $4\text{--}10\ \mu\text{mol N l}^{-1}$, generally higher in the order of June > September > March > December. No consistent temporal pattern was observed in TN (Fig. 5e); however, temporal variability was generally larger in June and September than in December and March. Total P con-

centration was usually $0.15\text{--}0.25\ \mu\text{mol P l}^{-1}$, and no seasonal trend was observed. No consistent temporal pattern was observed for TP (Fig. 5f).

Differences in nutrient concentrations between the five zones were evaluated by ANOVA followed by Scheffe's post-hoc multiple comparisons ($\alpha = 0.05$). Concentration of NO_3^- (Fig. 3) adopted significantly higher values in zones H and S (mean, 0.57 and $0.52\ \mu\text{M}$, respectively) than zones B and W (0.36 and 0.37), with median values in zone G (0.44). NO_2^- (range, $0.03\text{--}0.16\ \mu\text{M}$) was significantly higher in zones H and G (mean, 0.084 and 0.095) than zones B, S, W (0.057 , 0.070 , 0.074). NH_4^+ ($0.04\text{--}1.07\ \mu\text{M}$) was significantly lower in zone B (mean, 0.16) than zones S, W, H, G (0.22 , 0.23 , 0.23 , 0.29). PO_4^{3-} (Fig. 4) was significantly lower in zones W and G (mean, 0.046 and $0.048\ \mu\text{M}$) than zones S, B, H (0.063 , 0.063 , 0.066). TN (range, $3.6\text{--}13.8\ \mu\text{mol N l}^{-1}$) was significantly higher in zone G (mean, 8.5) and lower in zone B (5.7) than zones H, W, S (6.6 , 7.0 , 7.0). TP (range, $0.07\text{--}0.21\ \mu\text{mol P l}^{-1}$) was significantly higher in zone G (mean, 0.21) and lower in zone W (0.17) than zones H, B, S (0.19 , 0.19 , 0.20). Comparisons that are not mentioned above were statistically insignificant. Thus,

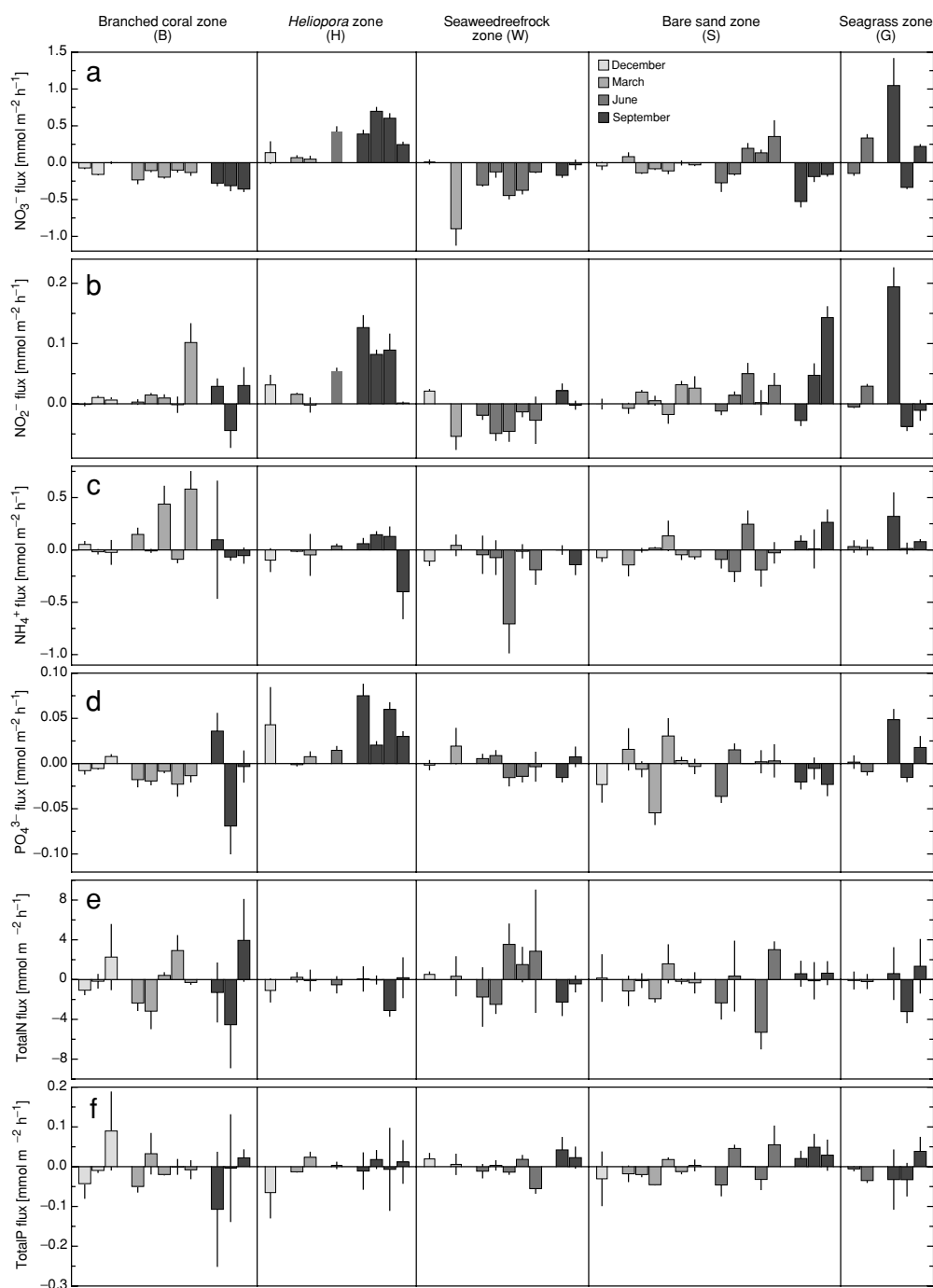


Fig. 5. Nutrient fluxes per unit bottom area (bars) and associated standard errors (error bars) estimated by individual drogue-tracking experiments for five zones defined in Fig. 2. From top to bottom: a, NO_3^- ; b, NO_2^- ; c, NH_4^+ ; d, PO_4^{3-} ; e, Total N; f, Total P. Colors of the bars indicate survey months (from thin to thick: December 1998, March 1999, June 1999, September 1999).

nutrient environment was relatively rich in zone H and more oligotrophic in zones B and W.

Net exchange rates of NO_3^- and NO_2^- were weakly correlated to each other ($r = 0.763$, $p < 0.0001$). In some

cases, NO_3^- net exchange rates showed negative correlation with NO_3^- concentration. In zone B, NO_3^- exchange measured in winter was correlated with NO_3^- concentration ($p = 0.0081$; Fig. 6a), while that measured in zone W

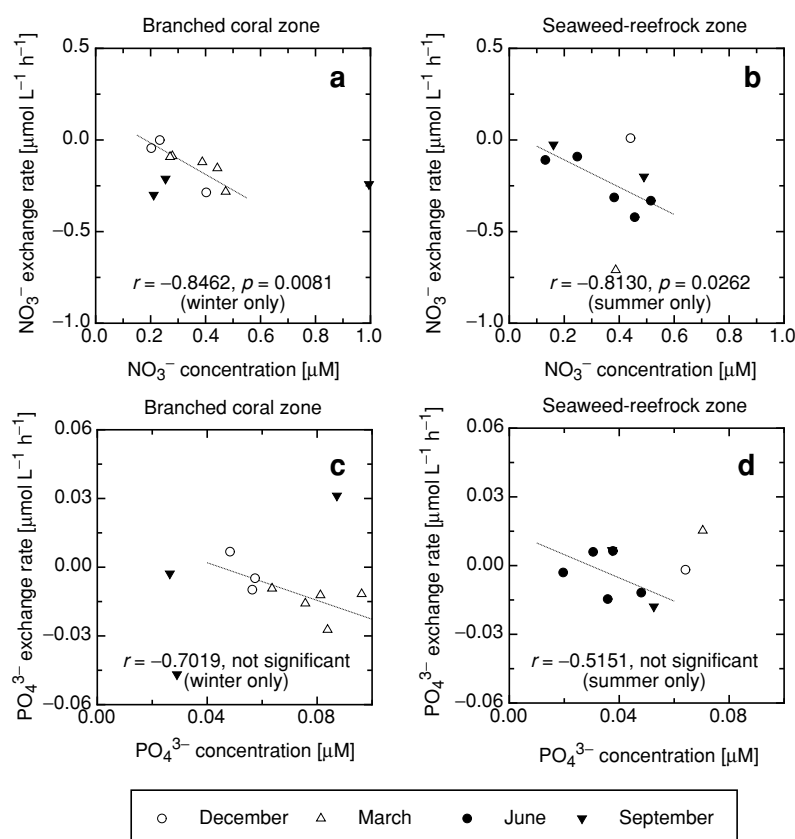


Fig. 6. Correlations between ambient concentrations and net exchange rates of NO_3^- (a, b) and PO_4^{3-} (c, d) observed in the branched coral zone (B in Fig. 2; a, c) and the seaweed-reefrock zone (W in Fig. 2; b, d). Linear regression lines and correlation coefficients are shown for winter data (December and March) of zone B and summer data (June and September) of zone W.

correlated with concentration only in summer ($p = 0.0262$; Fig. 6b). These correlations diminished when year-round data were included. Although statistically insignificant, a similar trend was also suggested for correlation between PO_4^{3-} net exchange and concentration (Figs. 6c and d). However, concentration dependence was not confirmed for net exchange rates of NO_2^- , NH_4^+ , TN and TP. NO_3^- exchange rate in zone B (year-round) and zone W (summer), as well as PO_4^{3-} exchange rate in zone W (summer) showed very weak, negative correlation with water flow rate (statistically not significant).

Si(OH)_4 , measured only in September (Fig. 4), was between 1 and 2 μM , being relatively higher during the first half of the survey period (Sep. 23 and 24; S2–S7) than during the last half (Sep. 28 and 29; S8–S15). Si(OH)_4 was considerably stable during individual experiments, and difference between zones was relatively small. These facts suggest that Si(OH)_4 levels in this lagoon were largely determined by the concentration in the inflowing seawater from the outer ocean, and that the influence of internal biogeochemical processes on Si(OH)_4 was ap-

parently small. Influence of groundwater, which contained ca. 130 μM of Si(OH)_4 (concentration at the freshwater-end on the concentration-salinity regression line), on the lagoon water chemistry was also apparently negligible. Si(OH)_4 and its flux were not examined further, due to limited data.

3.3 Contributions of planktonic processes

Nutrient exchanges by the planktonic microbial community, as estimated by the bottle incubation method, are shown in Table 2 (negative values mean net uptake). On average, net uptake of nutrients was observed in the light bottles (except PO_4^{3-} in March and NO_2^- in September), while net nutrient regeneration was detected in the dark bottles (except NO_2^- and NH_4^+ in March). Exchange rates in the light bottles were more negative than the corresponding rates in the dark bottles (except NO_2^- in March). The rates observed in the incubated bottles, either positive or negative, were 1–3 orders of magnitude lower than the net exchange rates observed during the drogoue-track experiments, even when the variability in planktonic mi-

Table 2. Nutrient exchange rates observed during *in-situ* bottle incubation of lagoon seawater. Unit of values is $\mu\text{mol L}^{-1} \text{h}^{-1}$. Presented data are the averages \pm standard errors or ranges of variation. Positive and negative rates mean net release and uptake of nutrients, respectively.

Month of 1999		Net exchange rates observed during the bottle incubation of lagoon water	
		Light ^(a)	Dark ^(b)
March	NO_3^-	-0.0004 ± 0.0049	0.0007 ± 0.0011
	NO_2^-	-0.0001 ± 0.0001	-0.0002 ± 0.0001
	NH_4^+	-0.0319 ± 0.0017	-0.0305 ± 0.0008
	PO_4^{3-}	0.0010 ± 0.0002	0.0015 ± 0.0001
June	NO_3^-	-0.0133 ± 0.0019	0.0008 ± 0.0009
	NO_2^-	-0.0010 ± 0.0002	0.0008 ± 0.0002
	NH_4^+	-0.0172 ± 0.0015	0.0130 ± 0.0022
	PO_4^{3-}	-0.0008 ± 0.0001	0.0003 ± 0.0005
September	NO_3^-	-0.0042 ± 0.0005	0.0008 ± 0.0005
	NO_2^-	0.0004 ± 0.0002	0.0010 ± 0.0001
	NH_4^+	-0.0113 ± 0.0009	0.0004 ± 0.0012
	PO_4^{3-}	-0.0008 ± 0.0002	0.0000 ± 0.0003

^(a)Bottles were incubated under *in-situ* light conditions from 09:00 to 17:00 local time ($n = 6-12$).

^(b)Bottles were covered with aluminum foils to keep dark and incubated *in situ* from 09:00 to 17:00 local time ($n = 6$).

crobal density (represented by Chl.*a*, ranging 0.1–0.8 $\mu\text{g l}^{-1}$) was accounted for. The fact that total net fluxes were 1–3 orders of magnitude larger than the corresponding water-column net fluxes is consistent with previous reports from other reefs (Hopkinson *et al.*, 1987; Sorokin, 1990). Therefore, as a first approximation, nutrient exchange observed during the drogoue-tracking experiments can be interpreted without referring to planktonic metabolisms.

3.4 Spatial correlations between nutrient exchange rates and benthic characteristics

The effects of benthic populations, physical conditions and ambient nutrient concentrations on net nutrient exchange rates were evaluated by stepwise multiple regression analysis (MRA). Results for NO_3^- , NO_2^- , NH_4^+ and PO_4^{3-} are shown in Table 3. The fraction of variation accounted for by the selected variables (r^2 value) was small for NH_4^+ and PO_4^{3-} (<30%) compared to NO_3^- and NO_2^- (>40%).

Dependence of the net exchange rates on physical and chemical variables was generally weak or absent. However, the exchange rate of NO_2^- was most strongly dependent on concentration of NO_3^- . Exchange rate of NH_4^+ was also correlated with concentrations of NO_3^- (positive) and NH_4^+ itself (negative), but the correlations were weak. Among benthic variables, areal biomass of the octocoral *Heliopora* showed a strong positive corre-

lation with exchange rates of NO_3^- , NO_2^- and PO_4^{3-} . In contrast, areal coverage of reefrocks was negatively correlated with these rates. Seagrass areal biomass showed a positive correlation with the exchange rates of 3 nitrogenous nutrients, though correlations were weak. These relationships between benthic characteristics and nutrient exchange rates were generally consistent with the findings derived from the zonal differences in exchange rates (Fig. 5).

MRA was also applied to the net exchange rates of TN and TP. However, no independent variable was proved to have a significant correlation with these rates.

4. Discussion

4.1 Ranges of nutrient exchange rates in reef-flat ecosystems

Coral reefs usually develop in nutrient-depleted coastal environments, and typical concentrations of dissolved inorganic nitrogen (DIN), phosphorus (DIP) and silicate are in the range of 0.5–4 μM , 0.05–0.5 μM and 1–3 μM , respectively (D'Elia, 1988; D'Elia and Wiebe, 1990). Concentration levels observed in the present study were generally within these ranges.

Several studies have estimated net nitrogen (N) exchange rates between coral reefs and seawater flowing over the reefs. For example, Webb *et al.* (1975) estimated net N exchange rates in a few transects of Enewetak At-

Table 3. Coefficients of multiple regression of the exchange rates of nitrate, nitrite, ammonium and phosphate during the drogue-tracking experiments ($n = 48$) to physicochemical and biological conditions that were proved to have significant correlation by the stepwise multiple regression analysis ($y = \sum a_i x_i + b$; entry criterion: $F > 4$; removal criterion: $F < 3$).

Exchange rates (y)	Independent variables (x_i)	Regression coefficient ($a_i \pm$ S.E.)	F
NO ₃ ⁻ [nmol l ⁻¹ h ⁻¹] $r^2 = 0.480$ $p = 0.0001$ $b = -744 \pm 471$	<i>Heliopora</i> biomass [mmol-N m ⁻³]	2.80 ± 0.52	29.2
	Reefrock coverage [m ⁻¹]	-355 ± 108	10.8
	Seagrass biomass [mmol-N m ⁻³]	9.4 ± 3.0	9.8
	Photosynthetically available radiation [μ mol m ⁻² s ⁻¹]	-0.29 ± 0.12	5.8
	Water temperature [°C]	37.5 ± 18.8	4.0
NO ₂ ⁻ [nmol l ⁻¹ h ⁻¹] $r^2 = 0.410$ $p = 0.0006$ $b = 3 \pm 13$	NO ₃ ⁻ concentration [μ M]	70.9 ± 21.2	11.2
	<i>Heliopora</i> biomass [mmol-N m ⁻³]	0.24 ± 0.07	11.0
	Reefrock coverage [m ⁻¹]	-46.7 ± 15.2	9.5
	Seagrass biomass [mmol-N m ⁻³]	1.05 ± 0.38	7.5
	Branched coral biomass [mmol-N m ⁻³]	0.17 ± 0.07	6.0
NH ₄ ⁺ [nmol l ⁻¹ h ⁻¹] $r^2 = 0.232$ $p = 0.0259$ $b = -9 \pm 70$	NO ₃ ⁻ concentration [μ M]	360 ± 145	6.1
	NH ₄ ⁺ concentration [μ M]	-868 ± 414	4.4
	Branched coral biomass [mmol-N m ⁻³]	0.62 ± 0.32	3.9
	Seagrass biomass [mmol-N m ⁻³]	3.19 ± 1.82	3.1
PO ₄ ³⁻ [nmol l ⁻¹ h ⁻¹] $r^2 = 0.272$ $p = 0.0219$ $b = -86 \pm 52$	<i>Heliopora</i> biomass [mmol-P m ⁻³]	3.04 ± 1.10	7.6
	Reefrock coverage [m ⁻¹]	-27.8 ± 11.3	6.0
	Bare sand coverage [m ⁻¹]	-51.2 ± 25.5	4.0
	Water temperature [°C]	3.36 ± 1.71	3.9
	PO ₄ ³⁻ concentration [μ M]	352 ± 182	3.7

oll, and according to their data, the rate ranges between -0.42 and +0.43 mmol-N m⁻² h⁻¹ for dissolved inorganic nitrogen (DIN), and between +0.07 and +0.91 mmol N m⁻² h⁻¹ for organic nitrogen (positive value means export to seawater, normalized to the bottom area). Andrews and Müller (1983) estimated regenerative export flux of DIN at a patch reef of Davies Reef to be ca. 0.71 mmol-N m⁻² h⁻¹. Estimates of net DIN and TN exchange rates in the present study (Figs. 5a, b, c and e) mostly fell within ± 0.6 and ± 3.0 mmol-N m⁻² h⁻¹, respectively.

On the other hand, Pilson and Betzer (1973) estimated net exchange rates of PO₄³⁻ and dissolved organic phosphorus (DOP) in Enewetak Atoll to be -0.088 to +0.016 and -0.038 to +0.054 mmol-P m⁻² h⁻¹, respectively. Net export flux of PO₄³⁻ estimated by Andrews and Müller (1983) at Davies Reef is about 0.024 mmol-P m⁻² h⁻¹, while net exchange rate of PO₄³⁻ estimated by Atkinson (1987) at Kaneohe Bay barrier reef is -0.018 mmol-P m⁻² h⁻¹ (i.e. net uptake). Most of the estimated net exchange rates of PO₄³⁻ and TP at Shiraho reef flat (Figs. 5d and f) were within the ranges of these previous

estimates.

Considering these estimates and other reports (Johannes *et al.*, 1983; Charpy *et al.*, 1998; Mioche and Cuet, 1999; Mwashote and Jumba, 2002; Baird *et al.*, 2004), it may be expected that reef-flat communities have a capacity to exchange DIN and PO₄³⁻ with overlying water at rates of around ± 0.6 and ± 0.05 mmol m⁻² h⁻¹, respectively. Organic phosphorus exchange is presumably of a similar magnitude to PO₄³⁻ flux. Organic nitrogen exchange, on the other hand, can be several times larger than DIN exchange, reflecting higher concentration of organic N than DIN in tropical surface waters (Miyajima *et al.*, 2007).

This study demonstrated that spatial correlations of nutrient exchange rates over the shallow reef flat ecosystem could be evaluated by the GIS-assisted flow-tracking method. In contrast to the previous flow-respirometric approaches, the present method also allowed a quantitative comparison of relative influence among individual benthic characteristics and physico-chemical conditions. However, although the flux of NO₃⁻ could be success-

fully determined in most cases, flux measurement of the other nutrients was sometimes problematic. Exchange rates of NO_2^- and PO_4^{3-} were often so small that temporal changes of their concentrations during a single drogue experiment were only marginally detectable or even undetectable by the instrumental analytical method used in this study. Contamination during sample handling was another problem for precise determination of temporal changes of nutrient concentrations, especially NH_4^+ . Relatively large standard errors for estimation of exchange rates of NH_4^+ and TN (Figs. 5c and e) are thought to be particularly ascribed to sample contamination. In addition, temporal variations in TN and TP concentrations were apparently confounded by interference of particulate N and P, such as coral mucus and resuspended sediment. Thus, there are several items in this method to be improved in the future for more precise determination of nutrient exchange rates in such oligotrophic aquatic systems.

4.2 Spatial variability and correlation in nutrient exchange rates

The variability in net nutrient exchange rates as determined by the proposed method may actually be caused by multiple mechanisms: (i) uptake and release of nutrients by the benthic biota over which the water mass passes; (ii) hydraulic leaching of nutrient-rich interstitial water from porous substrates (Andrews and Müller, 1983; Burnett *et al.*, 2003); (iii) production and consumption of nutrients by planktonic microorganisms conveyed with the water mass; and (iv) turbulent mixing of the water mass with neighboring water masses that have different nutrient concentrations. However, contribution of planktonic processes to overall nutrient fluxes has been shown to be relatively minor (Table 2), and the short turnover time of seawater (ca. 3 h) during high-tide periods precludes the development of local dense patches of phytoplankton in this reef flat. Therefore, mechanism (iii) can be excluded as a cause of spatial variabilities of nutrient distribution and fluxes. Mechanism (iv) is of secondary importance, as it requires the presence of neighboring water masses with different nutrient concentrations, which should already have been formed as a result of any of the other mechanisms. Therefore, mechanisms (i) and (ii) are the principal mechanisms to be considered here.

4.2.1 Branched-coral and seaweed-reefrock communities

Figures 3–5 showed that nutrients such as NO_3^- , NO_2^- and PO_4^{3-} were absorbed more actively by branched-coral and seaweed-reefrock communities than by *Heliopora* and bare-sand communities. MRA (Table 3) also showed that the net exchange rates of NO_3^- , NO_2^- and PO_4^{3-} were positively correlated with *Heliopora* den-

sity (i.e. more regenerative) and negatively correlated with reefrock coverage (more absorptive). This tendency is consistent with the mass transfer limitation model of nutrient uptake by sessile benthic organisms (Hearn *et al.*, 2001; Atkinson and Falter, 2003). Because the branched corals have more complex morphology and rougher surfaces than *Heliopora*, mass transfer rate should be higher for the former than the latter if the other conditions such as flow velocity and concentrations are same. Moreover, as the reefrock-covered area is generally shallower and has a more complex bottom morphology than bare sand area, water turbulence and therefore the mass transfer should be enhanced in the reefrock area. These factors are presumably responsible for the higher nutrient uptake by the branched-coral and seaweed-reefrock communities. The fact that none of the exchange rates showed a significant correlation with water flow velocity (Table 3) may be in apparent conflict with the model. The absence of this correlation may be explained by the fact that water flow velocity was not so different between experiments ($12.0 \pm 5.3 \text{ cm s}^{-1}$; mean \pm SD) as to significantly affect the mass transfer efficiency of nutrients.

Net nutrient absorption in the seaweed-reefrock community was enhanced in June (Fig. 5). Net uptake fluxes of NO_3^- and PO_4^{3-} in this area in summer (June and September) correlated with ambient concentrations of them, respectively (Figs. 6b and d). As dominant macroalgae such as *Sargassum* spp. grow from early spring and disappear in autumn, these facts again indicate that this absorption was particularly ascribed to macroalgal nutrient uptake and that the latter was limited by mass-transfer rates of nutrients. Epilithic microalgae, crustose coralline algae and algal turfs on gravels, which frequently occur in this area, might also have contributed to the observed fluxes, although seasonal changes in their abundance seemed less pronounced than the brown macroalgae. Concentration dependence of uptake fluxes of NO_3^- and PO_4^{3-} observed in the branched coral zone in winter (December and March; Figs. 6a and c) also suggest that nutrient uptake by these corals was mass-transfer limited. Using linear regression of net uptake rates (normalized to bottom area) with ambient concentrations, the uptake rate coefficient for NO_3^- in the branched coral zone (winter) and the seaweed-reefrock zone (summer) could be estimated as 0.59 ± 0.17 and $0.67 \pm 0.30 \text{ m h}^{-1}$, respectively (\pm standard error). These figures are similar to the NO_x^- uptake coefficient estimated at Warraber Island reef flat (0.44 – 0.51 m h^{-1} ; Baird *et al.*, 2004), although the estimation method is different. The PO_4^{3-} uptake rate coefficient in the branched coral zone (winter) was similarly calculated to be $0.46 \pm 0.15 \text{ m h}^{-1}$.

On the other hand, the fact that net absorption of NH_4^+ was often observed in the seaweed-reefrock zone but not in the branched coral zone (Fig. 5c) may be as-

cribed to low NH_4^+ concentrations in the latter zone (mean, $0.16 \mu\text{M}$) compared to NO_3^- in the same zone (mean, $0.36 \mu\text{M}$) and NH_4^+ in the former zone (mean, $0.23 \mu\text{M}$). This possibility is also supported by the MRA results (Table 3), which showed a net exchange rate of NH_4^+ correlated negatively with NH_4^+ concentration; viz., concentration-dependent NH_4^+ uptake. In addition, the exchange rates of NO_2^- and NH_4^+ were positively correlated with NO_3^- concentration. This may imply that NO_2^- and NH_4^+ were produced at the expense of NO_3^- in the course of assimilative nitrate reduction by primary producers. If this is true, then it would be difficult to estimate NH_4^+ uptake rates from the observed net exchange rates, especially when NO_3^- is more abundant than NH_4^+ .

4.2.2 *Heliopora*-dominated community

The fact that NO_3^- and PO_4^{3-} often increased when the drogue trajectory passed over the *Heliopora* community (Figs. 3 and 4) suggests that net regeneration of nutrients occurred within this community. Since seawater flows over the reef flat from north to south (as illustrated by H-1 and H-4 in Fig. 2) during most of the year except the summer months, organic matter such as coral mucus and detritus produced in the branched-coral and seaweed-reefrock communities may be continually transported to and accumulated in the downstream *Heliopora* community. Accumulation of organic matter in reef sediments results in higher DIN and PO_4^{3-} concentrations in pore waters through microbial remineralization, which in turn increase nutrient efflux to the overlying water (Corredor and Morell, 1985; Capone *et al.*, 1992; Miyajima *et al.*, 1998). Nutrient efflux was apparently enhanced in summer (June and September; Fig. 5), which may possibly be ascribed to temperature-dependent seasonal changes in sediment microbial activities. The efflux ratio of NO_3^- to PO_4^{3-} in summer was in the range 5.2 to 34 with a mean of 17.4. On the other hand, $\text{NO}_3^-/\text{PO}_4^{3-}$ concentration ratio in pore waters ranged from 1.1 to 8.5 (unpublished data; measured for top 10 cm sediment cores ($n = 4$) collected near the reference point A on September 1997 and 1998). This difference suggests that some additional sources other than sediment pore water supplied NO_3^- to seawater in this area. Nitrification in algal beds (Webb and Wiebe, 1975), coral skeleton (Wafar *et al.*, 1990) and benthic filter feeders (Diaz and Rützler, 2001) might have contributed to the observed NO_3^- loading. In addition, possible submarine discharge of groundwater with a high $\text{NO}_3^-/\text{PO}_4^{3-}$ ratio (ca. 1,000) cannot be ruled out, though we have no direct evidence.

Regardless of the underlying mechanism, the *Heliopora* community apparently has a “heterotrophic” nature in which regeneration rather than assimilation of inorganic nutrients prevails and, as a result, nutrient conditions are relatively rich. It is also possible that *Heliopora*, which may be an inferior competitor to the

branched corals for nutrient acquisition due to its simpler morphology and smoother surfaces, may prefer such environments where nutrient availability is originally high for some hydrographic reason. The low larval dispersability of this species (Harri and Kayanne, 2003) may also relate to this site preference. On the other hand, it has been shown that *Heliopora* has higher tolerance to elevated temperature than the branched corals (Kayanne *et al.*, 2002). Thus, given that nutrient requirement is met, *Heliopora* can be a superior competitor to the branched corals in regions where elevated temperature occasionally damages reef corals. These considerations imply that the more positive (i.e. regenerative) nutrient exchange rates observed in the *Heliopora* zone than the other zones are a cause rather than a result of the prevalence of *Heliopora* in this area. The *Heliopora* population in Shiraho Reef is one of the world’s largest colonies of this octocoral. The suggested high nutrient availability in this zone is presumably an important factor for maintenance of this population.

4.2.3 Bare sand area and seagrass beds

Nutrient exchange rates in the bare sand area were relatively small and showed no seasonal trend, though ambient nutrient concentrations were similar in range to the other zones (Figs. 3–5). The major nutrient sink in the bare sand zone is uptake by epipsamic microalgae (mainly diatoms and cyanobacteria), while the major source is bacterial remineralization of sedimentary organic matter. Although potential uptake rates of DIN and PO_4^{3-} by epipsamic algae are very high, nutrient demands for these algae can be met by diffusional nutrient supply from the pore water (Miyajima *et al.*, 2001; Suzumura *et al.*, 2002), and as a result, N and P cycles can be largely closed within the vicinity of the sediment/water interface. This is presumably the reason for the small exchange rates observed in this zone. However, since the abundance of some epipsamic algae, such as large filamentous cyanobacteria, is highly variable both in space and time, the source-sink balance for N and P can be disturbed locally. This is probably responsible for the observed variability in nutrient exchange rates in this zone.

The exchange rates of all the nitrogenous nutrients showed a weak positive correlation with the abundance of seagrasses (Table 3), which suggests that seagrass beds are also a site of nutrient regeneration, at least for N. Miyajima *et al.* (2001) have shown that there was a large pool of NH_4^+ (up to $400 \mu\text{M}$) in the pore water of the seagrass bed sediment, and that this NH_4^+ pool increased and NH_4^+ was emitted into the overlying water in summer. NH_4^+ emission was not observed in winter or in sediments of the bare sand zone, and NO_3^- was absorbed from the overlying water to the seagrass-bed sediment in both summer and winter (Miyajima *et al.*, 2001). Since the drogue experiment was carried out in the seagrass zone

mainly in summer (Figs. 3–5), it is probable that pore-water NH_4^+ emission from seagrass bed sediment affected the estimated NH_4^+ exchange rates. On the other hand, the abrupt increase of NO_3^- and $\text{Si}(\text{OH})_4$ observed during drogue experiments across the seagrass zone (J13 and S5 in Figs. 3 and 4) may have been due to direct mixing of groundwater from the shoreline to the water mass being tracked.

4.3 Comparison between biotic and abiotic factors

Primary production in oligotrophic aquatic ecosystems such as coral reefs is usually nutrient-limited, and therefore it may be supposed that the rates of nutrient uptake by reef organisms depend linearly on mass-transfer rates of nutrients. In fact, many previous studies of nutrient metabolisms of reef organisms at population or community levels have confirmed the mass-transfer limitation of nutrient acquisition (reviewed by Atkinson and Falter, 2003). This relationship means that nutrient dynamics in the reef benthic communities are principally constrained by abiotic factors such as water flow velocity, wave energy inputs and nutrient concentrations in inflowing offshore waters.

On the other hand, the present study has documented that, when spatial variability of nutrient dynamics on the reef flat was evaluated, nutrient exchange rates between reef biota and overlying water were constrained more strongly by the type of benthic biota than ambient nutrient concentration and water flow velocity (Table 3). Moreover, the dependence of nutrient exchanges on water temperature and light condition was weak (NO_3^- , PO_4^{3-}) or absent (NO_2^- , NH_4^+), which indicates that seasonal variation of the exchange rates was of relatively minor importance compared to differences between communities. Based on observed spatial variations of nutrient exchange rates (Figs. 3–5), the reef benthic biota can be classified into: (i) adsorption-dominated, or “autotrophic” community (branched coral and seaweed-reefrock communities); (ii) regeneration-dominated, or “heterotrophic” community (*Heliopora* community and seagrass beds); and (iii) nutritionally more closed community (bare-sand microalgal community). As for the “autotrophic” communities that occupy upstream regions in the water-flow regime of the study site, the mass-transfer limitation model of nutrient uptake was supported by the concentration dependence of net exchange rates of NO_3^- and PO_4^{3-} (Fig. 6). In particular, the magnitude of uptake rate coefficients for NO_3^- and PO_4^{3-} estimated from this relationship were of the same order as previous estimates at other natural and artificial coral communities (Atkinson and Falter, 2003; Baird *et al.*, 2004). For the other communities in downstream and near-shore regions, the overall nutrient dynamics were not apparently limited by mass-transfer rates.

The authors previously showed by a simple mass-balance model that the reef-flat ecosystem of Shiraho reef as a whole had a regenerative nature, exporting significant amounts of DIN and PO_4^{3-} to the adjacent outer ocean (Miyajima *et al.*, 2007). The present study suggests that this regenerative nature is mainly carried by the “heterotrophic” communities within the reef, such as *Heliopora* community and seagrass beds. Initial acquisition of N and P is accomplished by the “autotrophic” communities such as branched reef coral community and macroalgal beds, to which the mass-transfer limitation model can be applied. However, this relationship is obscured in the overall performance of the whole reef-flat ecosystem, because the “heterotrophic” communities play a pivotal role in nutrient dynamics.

In the previous paper we suggested that the regenerative trend as illustrated by this reef might be typical of high-latitude, subtropical reefs characterized by enhanced macroalgal production and high detrital flux. The present study showed that the macroalgal community in fact makes an important contribution to the reef-flat nutrient dynamics. Detrital organic matter containing N and P may be produced here, transported downstream to “heterotrophic” communities, and remineralized there by sediment microbial activities. Branched coral populations are also known to produce and export copious particulate organic matter as mucus (Coles and Strathmann, 1973; Coffroth, 1990), which potentially contributes to downstream heterotrophic activities. However, direct trophic linkage from the macroalgal and branched-coral communities to downstream “heterotrophic” communities has not yet been elaborated. Evaluation of detritus-based trophic linkages from “autotrophic” communities to downstream communities within an coral reef ecosystem is an important problem in understanding and characterizing ecosystem-level metabolisms of coral reefs and should be investigated in future studies.

Acknowledgements

This study was conducted as part of a multidisciplinary monitoring project for coral reef metabolism of the “CREST” program supported by Japan Science and Technology Agency from 1996 to 2001. Laboratory facilities at Ishigaki Island were kindly offered by Japan Sea-Farming Association, Yaeyama Station. The field survey was assisted by members of Shiraho Fishermen Cooperative. The drogue tracking system using GPS instruments was devised by K. Nozaki, K. Kato and A. Negishi (Energy Electronics Institute, AIST, Japan). Preparation of vegetation maps with the GIS program was assisted by M. Yamamuro (Institute of Marine Resource and Environment, AIST), M. Suzumura (Institute for Environmental Management Technology, AIST), S. Harii (Tokyo Institute of Technology), and staff of Fuyo Ocean

Development Corporation, Tokyo. Groundwater nutrient data were provided by Y. Tsuboi (Ocean Research Institute, The University of Tokyo). The authors benefited from many constructive comments by two anonymous reviewers on the earlier version of the manuscript.

References

- Andrews, J. C. and H. Müller (1983): Space-time variability of nutrients in a lagoonal patch reef. *Limnol. Oceanogr.*, **28**, 215–227.
- Atkinson, M. J. (1987): Rates of phosphorus uptake by coral reef flat communities. *Limnol. Oceanogr.*, **32**, 426–435.
- Atkinson, M. J. and R. W. Bilger (1992): Effects of water velocity on phosphate uptake in coral reef flat communities. *Limnol. Oceanogr.*, **37**, 273–279.
- Atkinson, M. J. and J. L. Falter (2003): Coral Reefs. p. 40–64. In *Biogeochemistry of Marine Systems*, ed. by K. D. Black and G. B. Shimmield, Blackwell Publishing, Oxford.
- Baird, M. E., M. Roughan, R. W. Brander, J. H. Middleton and G. J. Nippard (2004): Mass-transfer-limited nitrate uptake on a coral reef flat, Warraber Island, Torres Strait, Australia. *Coral Reefs*, **23**, 386–396.
- Barnes, D. J. (1983): Profiling coral reef productivity and calcification using pH and oxygen electrodes. *J. Exp. Mar. Biol. Ecol.*, **66**, 149–161.
- Barnes, D. J. and M. J. Devereux (1984): Productivity and calcification on a coral reef: a survey using pH and oxygen electrode techniques. *J. Exp. Mar. Biol. Ecol.*, **79**, 213–231.
- Bilger, R. W. and M. J. Atkinson (1995): Effects of nutrient loading on mass-transfer rates to a coral-reef community. *Limnol. Oceanogr.*, **40**, 279–289.
- Burnett, W. C., H. Bokuniewicz, M. Huettel, W. S. Moore and M. Taniguchi (2003): Groundwater and pore water inputs to the coastal zone. *Biogeochemistry*, **66**, 3–33.
- Burris, R. H. (1983): Uptake and assimilation of $^{15}\text{NH}_4^+$ by a variety of corals. *Mar. Biol.*, **75**, 151–155.
- Burton, J. D., T. M. Leatherland and P. S. Liss (1970): The reactivity of dissolved silicon in some natural waters. *Limnol. Oceanogr.*, **15**, 473–476.
- Bythell, J. C. (1990): Nutrient uptake in the reef-building coral *Acropora palmata* at natural environmental concentrations. *Mar. Ecol. Prog. Ser.*, **68**, 65–69.
- Capone, D. G., S. E. Dunham, S. G. Horigan and L. E. Duguay (1992): Microbial nitrogen transformations in unconsolidated coral reef sediments. *Mar. Ecol. Prog. Ser.*, **80**, 75–88.
- Charpy, L., C. Charpy-Roubaud and P. Buat (1998): Excess primary production, calcification and nutrient fluxes of a patch reef (Tikehau atoll, French Polynesia). *Mar. Ecol. Prog. Ser.*, **173**, 139–147.
- Coffroth, M. A. (1990): Mucus sheet formation on poritid coral: an evaluation of coral mucus as a nutrient source on reefs. *Mar. Biol.*, **105**, 39–49.
- Coles, S. L. and R. Strathmann (1973): Observations on coral mucus “flocs” and their potential trophic significance. *Limnol. Oceanogr.*, **18**, 673–678.
- Corredor, J. E. and J. Morell (1985): Inorganic nitrogen in coral reef sediments. *Mar. Chem.*, **16**, 379–384.
- Crossland, C. J. and D. J. Barnes (1983): Dissolved nutrients and organic particles in water flowing over coral reefs at Lizard Island. *Aust. J. Mar. Freshw. Res.*, **34**, 835–844.
- D’Elia, C. F. (1977): The uptake and release of dissolved phosphorus by reef corals. *Limnol. Oceanogr.*, **22**, 301–315.
- D’Elia, C. F. (1988): The cycling of essential elements in coral reefs. p. 195–230. In *Concepts of Ecosystem Ecology*, ed. by L. R. Pomeroy and J. J. Alberts, Springer, New York.
- D’Elia, C. F. and W. J. Wiebe (1990): Biogeochemical nutrient cycles in coral-reef ecosystems. p. 49–74. In *Coral Reefs*, ed. by Z. Dubinsky, Elsevier Science Publishers B.V., Amsterdam.
- Diaz, M. C. and K. Rützler (2001): Sponges: An essential component of Caribbean coral reefs. *Bull. Mar. Sci.*, **69**, 535–546.
- Falter, J. L., M. J. Atkinson and M. A. Merrifield (2004): Mass-transfer limitation of nutrient uptake by a wave-dominated reef flat community. *Limnol. Oceanogr.*, **49**, 1820–1831.
- Grasshoff, K., K. Kremling and M. Ehrhardt (1999): *Methods of Seawater Analysis*. Wiley, Weinheim.
- Harii, S. and H. Kayanne (2003): Larval dispersal, recruitment, and adult distribution of the brooding stony octocoral *Heliopora coerulea* on Ishigaki Island, southwest Japan. *Coral Reefs*, **22**, 188–196.
- Hata, H., S. Kudo, H. Yamano, N. Kurano and H. Kayanne (2002): Organic carbon flux in Shiraho coral reef (Ishigaki Island, Japan). *Mar. Ecol. Prog. Ser.*, **232**, 129–140.
- Hearn, C. J., M. J. Atkinson and J. L. Falter (2001): A physical derivation of nutrient-uptake rates in coral reefs: effects of roughness and waves. *Coral Reefs*, **20**, 347–356.
- Hopkinson, C. S., B. F. Sherr and H. W. Ducklow (1987): Microbial regeneration of ammonium in the water column of Davies Reef, Australia. *Mar. Ecol. Prog. Ser.*, **41**, 147–153.
- Johannes, R. E., W. J. Wiebe and C. J. Crossland (1983): Three patterns of nutrient flux in a coral reef community. *Mar. Ecol. Prog. Ser.*, **12**, 131–136.
- Kawahata, H., I. Yukino and A. Suzuki (2000): Terrestrial influences on the Shiraho fringing reef, Ishigaki Island, Japan: high carbon input relative to phosphate. *Coral Reefs*, **19**, 172–178.
- Kayanne, H., S. Harii, Y. Ide and F. Akimoto (2002): Recovery of coral populations after the 1998 bleaching on Shiraho Reef, in the southern Ryukyus, NW Pacific. *Mar. Ecol. Prog. Ser.*, **239**, 93–103.
- Mioche, D. and P. Cuet (1999): Métabolisme du carbone, des carbonates et des sels nutritifs en saison chaude, sur un récif frangeant soumis à une pression anthropique (île de la Réunion, océan Indien). *C. R. Acad. Sci. Paris Earth Planet. Sci.*, **329**, 53–59.
- Miyajima, T., I. Koike, H. Yamano and H. Iizumi (1998): Accumulation and transport of seagrass-derived organic matter in reef flat sediment of Green Island, Great Barrier Reef. *Mar. Ecol. Prog. Ser.*, **175**, 251–259.
- Miyajima, T., M. Suzumura, Y. Umezawa and I. Koike (2001): Microbiological nitrogen transformation in carbonate sediments of a coral-reef lagoon and associated seagrass beds. *Mar. Ecol. Prog. Ser.*, **217**, 273–286.
- Miyajima, T., H. Hata, Y. Umezawa, H. Kayanne and I. Koike (2007): Distribution and partitioning of nitrogen and phos-

- phorus in a fringing reef lagoon of Ishigaki Island, North-western Pacific. *Mar. Ecol. Prog. Ser.* (in press).
- Mwashote, B. M. and I. O. Jumba (2002): Quantitative aspects of inorganic nutrient fluxes in the Gazi Bay (Kenya): implications for coastal ecosystems. *Mar. Pollut. Bull.*, **44**, 1194–1205.
- Nakamori, T., A. Suzuki and Y. Iryu (1992): Water circulation and carbon flux on Shiraho coral reef of the Ryukyu Islands, Japan. *Cont. Shelf Res.*, **12**, 951–970.
- Odum, H. T. and E. P. Odum (1955): Trophic structure and productivity of a windward coral reef community on Eniwetok Atoll. *Ecol. Monogr.*, **25**, 291–320.
- Pilson, M. E. and S. B. Betzer (1973): Phosphorus flux across a coral reef. *Ecology*, **54**, 581–588.
- Sorokin, Yu. I. (1990): Plankton in the reef ecosystems. p. 291–327. In *Coral Reefs*, ed. by Z. Dubinsky, Elsevier Science Publishers B.V., Amsterdam.
- Sorokin, Yu. I. (1992): Phosphorus metabolism in coral reef communities: exchange between the water column and bottom biotopes. *Hydrobiologia*, **242**, 105–114.
- Steven, A. D. L. and M. J. Atkinson (2003): Nutrient uptake by coral-reef microatolls. *Coral Reefs*, **22**, 197–204.
- Suzumura, M., T. Miyajima, H. Hata, Y. Umezawa, H. Kayanne and I. Koike (2002): Cycling of phosphorus maintains the production of microphytobenthic communities in carbonate sediments of a coral reef. *Limnol. Oceanogr.*, **47**, 771–781.
- Tanaka, Y. and H. Kayanne (2006): Species composition of tropical seagrass meadow in relation to multiple physical environmental factors. *Ecol. Res.*, **22**, 87–96.
- Tanaka, Y., T. Miyajima, I. Koike, T. Hayashibara and H. Ogawa (2006): Translocation and conservation of organic nitrogen within the coral-zooxanthella symbiotic system of *Acropora pulchra*, as demonstrated by dual-isotope labeling techniques. *J. Exp. Mar. Biol. Ecol.*, **336**, 110–119.
- Thomas, F. I. M. and M. J. Atkinson (1997): Ammonium uptake by coral reefs: Effects of water velocity and surface roughness on mass transfer. *Limnol. Oceanogr.*, **42**, 81–88.
- Umezawa, Y., T. Miyajima, H. Kayanne and I. Koike (2002): Significance of groundwater nitrogen discharge into coral reefs at Ishigaki Island, Japan. *Coral Reefs*, **21**, 346–356.
- Wafar, M., S. Wafar and J. J. David (1990): Nitrification in reef corals. *Limnol. Oceanogr.*, **35**, 725–730.
- Webb, K. L. and W. J. Wiebe (1975): Nitrification on a coral reef. *Can. J. Microbiol.*, **21**, 1427–1431.
- Webb, K. L., W. D. DuPaul, W. Wiebe, W. Sottile and R. E. Johannes (1975): Enewetak (Eniwetok) Atoll: Aspects of nitrogen cycle on a coral reef. *Limnol. Oceanogr.*, **20**, 198–210.
- Wiebe, W. J. (1988): Coral reef energetics. p. 231–245. In *Concepts of Ecosystem Ecology*, ed. by L. R. Pomeroy and J. J. Alberts, Springer-Verlag, New York.